# Monohelical Complexes of a Novel Asymmetric $N_4$ Schiff Base: Unfamiliar Tetrahedral Environments of Manganese(II) and Iron(II) Helicates

**Miguel Vázquez,[a] Manuel R. Bermejo,*[a] Matilde Fondo,[a] Ana M. García-Deibe,[a] Jesús Sanmartín,[a] Rosa Pedrido,[a] Lorenzo Sorace,[b] and Dante Gatteschi[b]**

**Keywords:** Electrochemistry / Helical structures / Schiff bases / Transition metals

The electrochemical reaction of the bis-bidentate $H_2$ABATs Schiff base [$H_2$ABATs = *N*,*N'*-bis(2-tosylaminobenzylidene)-2-aminobenzylamine] with manganese, iron, cobalt, nickel, copper, zinc and cadmium was investigated. The reaction cell yields products of empirical formula M(ABATs). X-ray diffraction studies show that [Mn(ABATs)]·0.75$H_2O$ (**1**), [Fe(ABATs)]·0.75$H_2O$ (**2**), [Ni(ABATs)]·0.75$H_2O$ (**3**), [Cu(ABATs)]·0.5$H_2O$ (**4**) and [Zn(ABATs)]·0.75$H_2O$ (**5**) are mononuclear distorted tetrahedral helical complexes in the solid state. Complexes **1** and **2** confirm the ability of this type of ligand to dictate the geometry around the metal centre, as is shown by the unfamiliar tetrahedral environments of manganese(II) and iron(II) ions in complexation with the Schiff bases.

## Introduction

Molecular architectures featuring helical arrangements of multidentate ligands around one or more metal centres are one of the goals of supramolecular chemistry.[1−4] In this search, many studies have been performed in order to develop synthetic procedures for new multidentate ligands exhibiting the potential to give bridged polynuclear species.[5−11] Among the various ligand systems capable of promoting self-assembly of mononuclear and/or polynuclear helical coordination complexes, careful design of imine-based ligands[12−20] demonstrates that this can be an inexpensive approach to supramolecular chemistry. These ligands have the advantage of being easily modified, allowing changes in the features (length, flexibility, donor ability) of the spacer, the position of the donor atoms and the presence of different groups that can give rise to intermolecular interactions and/or induce torsion of the ligand. A systematic study of the factors affecting the isolation of helical complexes can therefore be done by changing just one of the variables.

We have recently prepared some bis-bidentate Schiff bases containing bulky tosyl groups and different spacers.[21−22] These ligands yield mononuclear and/or dinuclear helicates, depending on the flexibility and/or the length of the spacer, as well as on the nature of the metal atom. In fact, a Schiff base with a flexible propylene spacer separating the *N*-imine donors can give rise to complexes of different nuclearity, depending on the metal ion.

Regardless of the mono- or dinuclear nature of the helix, all complexes prepared with this kind of Schiff base show coordination numbers of four for the metal centres. It therefore seems that the stereochemical preferences of the metal do not play a fundamental role in the nuclearity of the complex in this case study. Until now, however, neither manganese(II) nor iron(II) complexes of this type had been crystallographically characterised, these metals having special preference for an octahedral coordination. To the best of our knowledge, in fact, no tetrahedral Schiff-base complexes with these metal atoms have been structurally characterised.

In an attempt to determine whether the presence of the tosyl groups can always dictate the geometry around the metal centre, and to examine the influence of the flexibility of the spacer on the nuclearity of the helix, the new $H_2$ABTs ligand (Scheme 1), with a semi-rigid benzylidene group (three carbon atoms) between the two imine moieties, was prepared. The interaction of $H_2$ABATs with manganese, iron, cobalt, nickel, copper, zinc and cadmium in an electrochemical cell was investigated and the results achieved are described.

## Results and Discussion

### Synthesis of the Ligand

The Schiff base $H_2$ABATs was prepared by conventional condensation between 2-tosylaminobenzaldehyde and 2-aminobenzylamine. The yellow solid showed a satisfactory

---

[a] Departamento de Química Inorgánica, Facultade de Química, Universidade de Santiago de Compostela,
15706 Santiago de Compostela, Spain
E-mail: qimb45@usc.es

[b] Dipartimento di Chimica, Universita degli Studi di Firenze, Polo Scientifico Universitario,
50099 Sesto Fiorentino (Fi), Italy

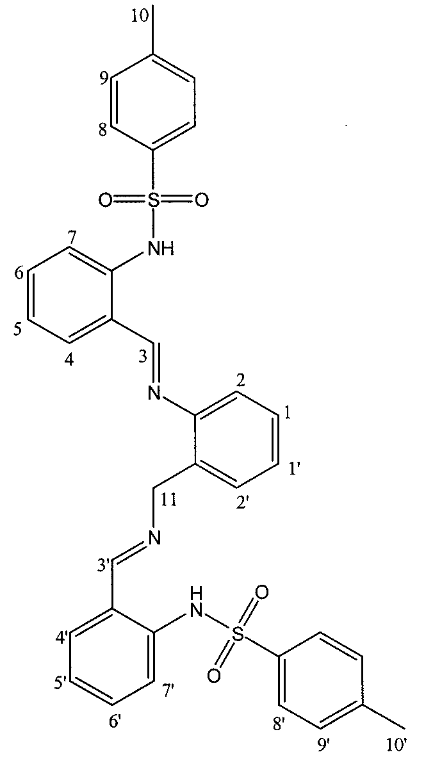

Scheme 1. $H_2ABATs$

elemental analysis and was further characterised by IR and $^1H$ NMR spectroscopy and FAB mass spectrometry.

### Electrochemical Synthesis of the Complexes

All the complexes were prepared by a previously described electrochemical method.[21]

Elemental analyses show that all metals employed here react with the ligand in a 1:1 molar ratio to afford complexes of the bis-deprotonated $[ABATs]^{2-}$ with high purity. All these neutral metal complexes are obtained in good yields and appear to be stable both in the solid state and in solution. It therefore seems that although an inert atmosphere is necessary for the isolation of pure manganese(II) and iron(II) complexes, these compounds are air-stable once formed.

### X-ray Studies

The crystal structures of $[Mn(ABATs)]\cdot0.75H_2O$ (**1**), $[Fe(ABATs)]\cdot0.75H_2O$ (**2**), $[Ni(ABATs)]\cdot0.75H_2O$ (**3**), $[Cu(ABATs)]\cdot0.5H_2O$ (**4**) and $[Zn(ABATs)]\cdot0.75H_2O$ (**5**) were solved as detailed below.

The five complexes are isomorphous and isostructural, and so only the ORTEP diagram of **1** is shown in Figure 1. Experimental details are recorded in Table 1 and the main bond distances and angles in Table 2.

### Metal-Ion Geometry

All the complexes consist of mononuclear compounds with water as solvate. In each case the ligand uses its four nitrogen atoms (two imine and two amide) to link to the metal atom. In addition, one oxygen atom of each tosyl group interacts weakly with the metal centre (Table 2). These distances are too long to be regarded as true coordinated bonds, and are better described as secondary intramolecular interactions. The metal centre is therefore in a tetracoordinated environment, with the tosyl groups playing an important role in the adopted coordination number. However, it is noteworthy that the higher preference for an octa-

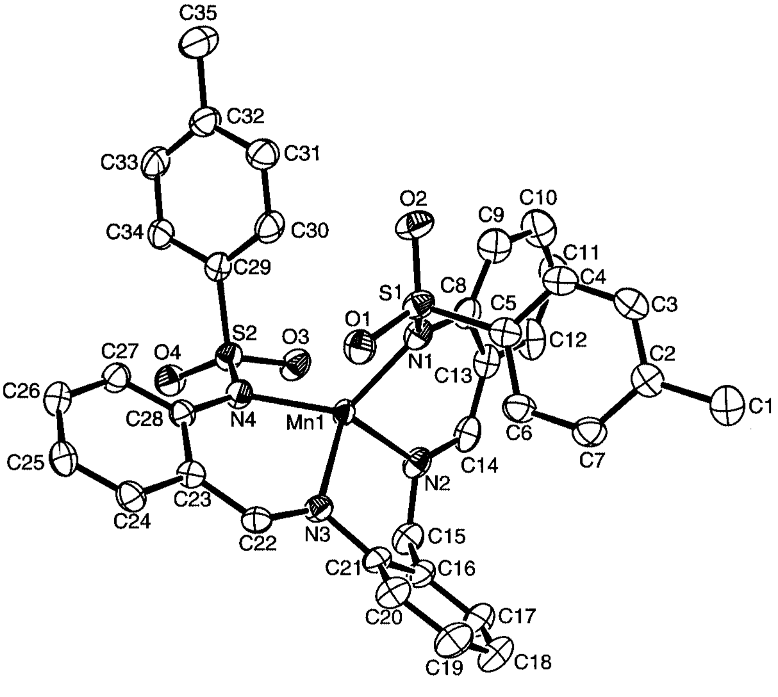

Figure 1. An ORTEP view of complex **1**, showing the *P* enantiomer (thermal ellipsoids are drawn at the 30% probability level; hydrogen atoms and solvent molecules have been omitted for clarity)

Table 1. Crystal data and structure refinement for **1−5**

| | **1** | **2** | **3** | **4** | **5** |
|---|---|---|---|---|---|
| Empirical formula | $C_{35}H_{31.50}MnN_4O_{4.75}S_2$ | $C_{35}H_{31.50}FeN_4O_{4.75}S_2$ | $C_{35}H_{31.50}NiN_4O_{4.75}S_2$ | $C_{35}H_{31}CuN_4O_{4.5}S_2$ | $C_{35}H_{31.50}ZnN_4O_{4.75}S_2$ |
| Molecular weight | 703.20 | 704.11 | 706.97 | 707.30 | 713.63 |
| Crystal system | Monoclinic | Monoclinic | Monoclinic | Monoclinic | Monoclinic |
| Space group | *P*2/*c* (No.13) | *P*2/*c* (No.13) | *P*2/*c* (No.13) | *P*2/*c* (No.13) | *P*2/*c* (No.13) |
| *a* (Å) | 19.486(3) | 19.51830(10) | 19.3080(5) | 19.207(5) | 19.296(3) |
| *b* (Å) | 10.696(2) | 10.6748(2) | 10.7143(3) | 10.636(4) | 10.736(2) |
| *c* (Å) | 17.636(3) | 17.6367(10) | 17.7497(4) | 17.760(5) | 17.755(4) |
| α (°) | 90 | 90 | 90 | 90 | 90 |
| β (°) | 114.74(2) | 114.8230(10) | 115.1580(10) | 114.98(2) | 114.823(13) |
| γ (°) | 90 | 90 | 90 | 90 | 90 |
| *V* (Å$^3$) | 3338.4(10) | 3335.2(2) | 3323.59(15) | 3288.7(18) | 3338.3(11) |
| Z | 4 | 4 | 4 | 4 | 4 |
| Absorption coefficient (mm$^{-1}$) | 0.568 | 0.625 | 0.757 | 0.838 | 0.908 |
| Crystal size (mm$^3$) | 0.25 × 0.15 × 0.10 | 0.20 × 0.10 × 0.05 | 0.40 × 0.25 × 0.15 | 0.40 × 0.25 × 0.15 | 0.40 × 0.25 × 0.10 |
| Reflections collected | 20493 | 17037 | 16931 | 16721 | 16789 |
| Independent reflections | 7647 [*R*(int) = 0.0367] | 7652 [*R*(int) = 0.0638] | 7625 [*R*(int) = 0.0585] | 7554 [*R*(int) = 0.0888] | 7607 [*R*(int) = 0.0371] |
| θ range (°) | 1.90−27.54 | 1.91−27.52 | 1.17−27.58 | 2.24−27.53 | 1.16−27.55 |
| Data/restraints/parameters | 7647/0/423 | 7652/0/429 | 7625/0/423 | 7554/0/419 | 7607/0/429 |
| Final *R* indices [$I > 2\sigma(I)$] | *R*1 = 0.0538 | *R*1 = 0.0698 | *R*1 = 0.0590 | *R*1 = 0.0774 | *R*1 = 0.0488 |
| | *wR*2 = 0.1153 | *wR*2 = 0.1456 | *wR*2 = 0.1570 | *wR*2 = 0.1539 | *wR*2 = 0.1100 |
| *R* indices (all data) | *R*1 = 0.0924 | *R*1 = 0.1422 | *R*1 = 0.1084 | *R*1 = 0.1705 | *R*1 = 0.0866 |
| | *wR*2 = 0.1329 | *wR*2 = 0.1765 | *wR*2 = 0.1863 | *wR*2 = 0.1944 | *wR*2 = 0.1325 |

Table 2. Selected bond lengths [Å] and angles (°) for 1−5

| | **1** | **2** | **3** | **4** | **5** |
|---|---|---|---|---|---|
| M(1)−N(1) | 2.047(3) | 2.029(4) | 1.989(3) | 1.978(4) | 1.990(3) |
| M(1)−N(2) | 2.053(2) | 2.056(3) | 1.961(3) | 1.940(4) | 2.015(3) |
| M(1)−N(3) | 2.091(3) | 2.096(3) | 2.000(3) | 1.977(4) | 2.045(2) |
| M(1)−N(4) | 2.017(2) | 2.008(3) | 1.937(3) | 1.956(4) | 1.962(2) |
| M(1)···O(1) | 2.680(2) | 2.634(3) | 2.828(3) | 2.765(4) | 2.763(2) |
| M(1)···O(3) | 2.595(2) | 2.519(3) | 2.552(2) | 2.647(4) | 2.681(2) |
| N(1)−M(1)−N(2) | 87.07(11) | 86.23(14) | 89.55(13) | 90.79(19) | 90.82(11) |
| N(1)−M(1)−N(3) | 132.97(10) | 132.22(14) | 126.27(12) | 136.85(19) | 130.14(11) |
| N(1)−M(1)−N(4) | 123.65(10) | 126.44(14) | 117.93(13) | 108.20(18) | 120.20(10) |
| N(2)−M(1)−N(3) | 92.18(10) | 91.80(14) | 94.50(13) | 94.53(19) | 92.36(10) |
| N(2)−M(1)−N(4) | 135.32(11) | 135.16(15) | 140.19(13) | 143.2(2) | 133.52(11) |
| N(3)−M(1)−N(4) | 88.15(10) | 86.41(13) | 91.26(12) | 92.43(18) | 91.83(10) |

hedral geometry is displayed in the shorter M···O$_{tosyl}$ distance.

The dihedral angle θ between the two MNN terminal planes (ca. 62.3° for **1**, 62.6° for **2**, 65.3° for **3**, 55.9 for **4** and 64.9° for **5**) shows that the metal ion displays a tetrahedral geometry with a square-planar distortion (θ = 0° for square-planar geometry and θ = 90° for tetrahedral geometry). The value of θ for **4** indicates that the geometry around the copper atom could in fact be viewed as intermediate between tetrahedral and square-planar. This geometry is quite unfamiliar for manganese(II) and iron(II) Schiff-base complexes, which display clear stereochemical preferences for octahedral environments, and even for Ni$^{II}$, which also prefers octahedral or square-planar rather than tetrahedral geometries. To the best of our knowledge, no manganese Schiff-base complexes with this geometry have been described previously, and just one iron(II) tetrahedral complex of a bidentate Schiff base ($FeL_2$) has recently been characterised.[23] Nevertheless, it should be noted that this complex was prepared in non-polar, non-coordinating solvents under an inert atmosphere. In our case the iron centre maintains its tetrahedral environment despite the presence of water in the solvent and trapped in the unit cell, which demonstrates the ability of this type of ligand to predetermine the coordination polyhedron. It therefore seems that the steric hindrance induced by the tosyl groups, in conjunction with the second order interactions of the metal with the tosyl oxygen atoms, prevent any other donor from coordinating to the metal ion.

In addition, it must be pointed out that Zn and Ni form dinuclear complexes with $H_2$PTs [*N*,*N*′-bis(2-tosylaminobenzylidene)-1,3-diaminopropane],[21] while they afford mononuclear compounds with $H_2$ABATs. The related $H_2$PTs ligand, like $H_2$ABATs, contains three carbon atoms between the imine moieties. However, the spacer in $H_2PTs$ is an aliphatic chain and this emphasises the role of the spacer flexibility in the nuclearity of the helix.

The M−N (M = Ni, Cu, Zn) distances are typical of tetracoordinate tetrahedral complexes,[21−22] but are shorter than those found for octahedral complexes with similar ligands,[24] reflecting the lower coordination number. The $M-N_{imine}$ (M−N2 and M−N3) distances decrease monotonically from **1** to **4** and increase for **5**, following the trend (**1** ≈ **2** > **5** > **3** > **4**) of the ionic radii. The $M-N_{amide}$ (M−N1 and M−N4) distances show the same pattern.

The wide range of angles observed around the metal centres, varying between ca. 87° and 143.2°, compares fairly well with those previously reported for this kind of complex and reflects the severe distortion from the ideal tetrahedral geometry.

### Chelate Rings and Helical Coiling

The ligand forms three chelate rings around the central metal atom. The two terminal six-membered rings are reasonably planar while the central six-membered ring is less so, as would be expected, due to the presence of one $sp^3$ carbon atom. The loss of planarity between the $N_{imine}$ atoms is also shown by the N(2)C(15)C(16)C(21) torsion angles, which range from −58.7(5)° for **3** to 63.0(4)° for **2**, showing the strain of the ligand. The central N(2)C(15)C(16)C(21)N(3) chelate ring forms angles of ca. 46° and 27° for **1**−**3** and **5** and of ca. 41° and 23° for **4** with N(1)C(8)C(13)C(14)N(2) and N(3)C(22)C(23)C(28)N(4), respectively. These angles show the screwing of this thread, which affords monohelical single-stranded molecules. The twisting of the ligand can be attributed to an attempt by the additional peripheral tosyl groups to minimise the steric hindrance, being orientated in different directions, as shown in Figure 2.

The extent of helical coiling in these chiral complexes can be described in terms of the ligand wrapping angle. However, the value of this angle, and of the helical pitch of the thread, can change significantly depending on different considerations, such as the actual helix top-ends or the helical axis declination, so only qualitative aspects are considered.

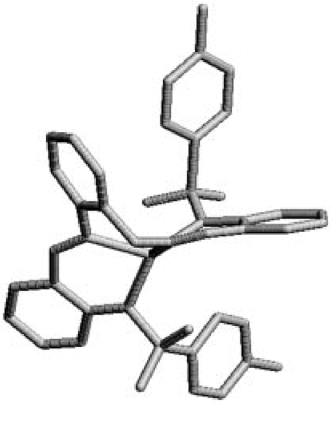

Figure 2. Stick view of **1**, showing the wrapping of the ligand

It can clearly be observed (Figure 2) that, if only the donor atoms are taken into account, the wrapping angle is always shorter than 360°. Nevertheless, if the tosyl groups are included, the ligand wraps slightly more than once. In that sense, the S···S distances could be taken as a close value for the pitch, being ca. 5.0 Å for **1**, 4.98 Å for **2**, 4.88 Å for **3**, 4.74 Å for **4** and 4.99 Å for **5**. These distances show that the shortest pitch corresponds to **4**, which is in agreement with its more distorted (tetrahedral towards square-planar) geometry.

Finally, the space group and the analysis of the crystal data indicate the formation of a racemic mixture, with both *P* and *M* enantiomers present in the unit cell with 50% yield for all the complexes.

### IR Spectra

The IR spectra of the free ligand and complexes show two bands at ca. 1605 and 1630 $cm^{-1}$, in agreement with the presence of two inequivalent imine groups. Both ν(C=N) bands are shifted to higher wavenumber values (1−15 $cm^{-1}$) with respect to the free ligand for most of the complexes. In addition, all complexes show a negative shift of ν(C−N) relative to free $H_2ABATs$. This suggests the coordination of the ligand to the metal centre through the imine and amide nitrogen atoms. In addition, two bands in the ranges 1250−1261 $cm^{-1}$ and 1127−1138 $cm^{-1}$ are attributable to the asymmetric and symmetric vibration modes of the $SO_2$ group, respectively.[25−26] Finally, no bands above 2500 $cm^{-1}$ were detected for any of the complexes, indicating the deprotonation of the NH groups and, therefore, the dianionic character of the ligand.

### Magnetic Studies

The magnetic moments of all the paramagnetic complexes were recorded in the solid state between 2 and 280 K. In agreement with the observed long distances between magnetic centres (ca. 9.5 Å), and with the absence of any efficient exchange pathway, the temperature dependence of the magnetic susceptibilities between 2 and 280 K for all the complexes shows deviation from Curie behaviour only at low temperature, with the exception of the $Ni^{II}$ complex for which, due to the expected partially unquenched orbital contribution, a deviation is observed below 50 K (Figure 3). The values of the magnetic moment, obtained by the Curie−Weiss fit of $1/\chi$ vs. $T$ plots (Table 3), are very close to those expected for magnetically diluted tetrahedral $M^{II}$ ions, with $g$ values that, except for $Mn^{II}$, differ greatly from that of the free electron.[27] This provides confirmation of the oxidation state +II for the metal centre, indicating the deprotonation of the Schiff-base ligand, and the achieved high-spin configuration for [Mn(ABATs)] and [Fe(ABATs)], as would be expected. The EPR spectra essentially confirm this picture; indeed, a typical tetrahedral $Cu^{II}$ spectrum is observed for the complex [Cu(ABATs)], which yielded $g$ values $g_{\|} = 2.185$ $g_{\perp} = 2.095$ with an average $g$ value of 2.125, in good agreement with the magnetic moment observed at room temperature. On the other hand, the EPR spectrum of the $Mn^{II}$ derivative, recorded at low temperature, clearly shows a fine structure deriving from a non-negligible zero field splitting (ZFS) of the $S = 5/2$ multiplet (Figure 4). Finally, no EPR spectra are observed for the $Fe^{II}$ and $Co^{II}$ derivatives: the absence of a spectrum for the former is in agreement with the expected large ZFS and integer spin state that usually make tetrahedral high-spin $Fe^{II}$ complexes silent at EPR X-band frequencies.[28] The non-observation of an EPR spectrum for the $Co^{II}$ derivative, a Kramers ion, could be attributable to fast relaxation.[29]

Thus, in view of the formulations of the complexes and their magnetic moments, it seems quite reasonable to propose a tetrahedral environment around the metal atoms for all the paramagnetic complexes, as the crystal structures of **1** to **5** confirm.

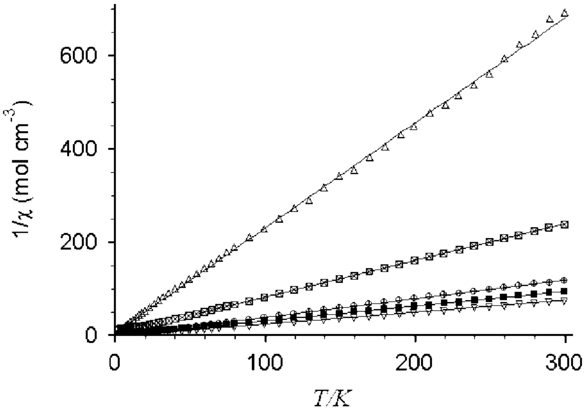

Figure 3. Curie−Weiss plots for paramagnetic complexes; Δ Cu derivative, □ Ni derivative, ○ Co derivative, ■ Fe derivative and ▽ Mn derivative

Table 3. Value of the Curie constant for the complexes

| Complex | $C$ ($cm^3 \cdot K \cdot mol^{-1}$) |
|---|---|
| Mn(ABATs) | 3.88 |
| Fe(ABATs) | 3.17 |
| Co(ABATs) | 2.5 |
| Ni(ABATs) | 1.28 |
| Cu(ABATs) | 0.44 |

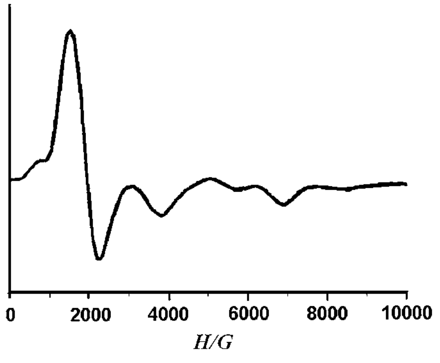

Figure 4. EPR band spectrum (at 9.225 GHz) of Mn(ABATs) recorded at 4.2 K

## FAB Mass Spectra

FAB mass spectra of all the complexes show peaks due to $[M(ABATs)]^+$ fragments (M = Mn, Fe, Co, Ni, Cu, Zn or Cd), corroborating the coordination of the ligand to the metal. However, no peaks attributable to $[ML]_2^+$ fragments could be detected for any of the complexes, suggesting mononuclear natures in solution for all of them.

## NMR Studies

The $^1H$ NMR spectra of $H_2ABATs$, [Zn(ABATs)] and [Cd(ABATs)] were recorded in $[D_6]DMSO$ as solvent. The spectra show two sets of aromatic signals in a 1:1 ratio, indicating that the two arms are not magnetically equivalent. The assignments of the signals were based on COSY and NOESY experiments, as well as on previous results.[21−22]

The comparison of the free ligand spectrum with those of the complexes allows some conclusions to be drawn:

1. The NH protons present in the free ligand disappear in the spectra of the complexes, in agreement with bis-deprotonation of the Schiff base.
2. The imine hydrogen atoms (3-H and 3′-H) show a shift to lower field for the zinc complex, while 3-H is shifted to higher field in the cadmium complex, indicating that the coordination of the imine groups to the metal centre induces opposite shielding effects on these hydrogen atoms. This situation was also found for zinc and cadmium complexes with ligands containing an aliphatic spacer.[21b]

The imine protons of the cadmium complex are flanked by satellites arising from spin-spin coupling to $^{111/113}Cd$, suggesting that the complex is kinetically inert on the NMR timescale.

3. The methylene protons (11-H) are magnetically equivalent in the free ligand and appear as a singlet at $\delta = 5.08$ ppm. However, the room-temperature spectrum of the zinc complex contains a well resolved AB doublet of doublets for the 11-H protons. The AB pattern for the methylene hydrogen atoms implies that the strong coordination of the hard imine nitrogen to the zinc atom abolishes the erstwhile enantiotopic nature of these protons to make them diastereotopic. This observation can be interpreted in terms of a helical conformation of the new complex, making it chiral. It therefore seems that the zinc complex in solution maintains the structure found in solid state.

The spectrum of the cadmium complex at room temperature shows just one broad signal at $\delta = 4.97$ ppm for the 11-H protons. This could indicate that the complex is not chiral or that a fast interconversion of enantiomers of the chiral single helicate takes place in solution.

Finally, it should be noted that just one diastereoisomer exists in solution for both complexes, as no additional peaks indicative of a second species could be detected.

## Conclusions

The electrochemical interaction of manganese, iron, cobalt, nickel, copper, zinc and cadmium with the bis-bidentate $H_2$ABATs Schiff base yields mononuclear [$M^{II}$(ABATs)] complexes. The bulky tosyl groups induce torsion in the ligand, giving rise to monohelical, single-stranded, tetrahedral compounds. This geometry is quite unusual for manganese(II) and iron(II) with Schiff bases. In fact, to the best of our knowledge, there are no previous crystallographically characterised examples of this type of complex obtained from non-anhydrous solvents. This demonstrates the ability of this type of ligand to dictate the coordination number in spite of the geometrical preferences of the metal.

Finally, this work further contributes to make the role of the flexibility of the spacer in the nuclearity of the helix evident: nickel and zinc double-helical compounds have previously been reported for a related ligand ($H_2$PTs) with a flexible propylene spacer (three aliphatic carbon atoms between imine-N atoms), while the semi-rigid benzylidene spacer in $H_2$ABATs (three carbon atoms, two aromatic and one aliphatic, between imine-N atoms) only allows the isolation of monohelical complexes.

## Experimental Section

**General:** Elemental analyses were performed on a Carlo Erba EA 1108 analyser. Infrared spectra were recorded as KBr pellets on a Bio-Rad FTS 175 spectrophotometer in the 4000−600 $cm^{-1}$ range. NMR spectra were recorded on a Bruker AMX 500 spectrometer in [$D_6$]DMSO as solvent. Fast atom bombardment (FAB) mass spectra were performed on a Kratos MS-50 mass spectrometer, employing Xe atoms at 70 keV in *m*-nitrobenzyl alcohol as matrix. EPR spectra were recorded on a Varian ESR9 spectrometer working at the X-band frequency (9.225 GHz) equipped with a $^4$He continuous flow cryostat for low temperature measurements. Magnetic measurements were performed between 2 and 280 K with a Cryogenics Squid S600 magnetometer with applied field of 1 T. The data were corrected for sample holder contribution and diamagnetism of the sample by the use of Pascal constants.

**Synthesis:** All the starting materials were purchased from Aldrich and used without further purification. 2-Tosylaminobenzaldehyde was prepared and characterised according to the literature.[30−31]

**Ligand Preparation:** 2-Aminobenzylamine (1.13 g, 9.1 mmol) was added to a solution of 2-tosylaminobenzaldehyde (5.0 g, 18.2 mmol) in chloroform (150 mL), and the mixture was heated to reflux. The volume of the solution was reduced to ca. 50 mL over a 4 h period with the aid of a Dean−Stark trap, and the mixture was then allowed to cool. The resultant yellow solution was concentrated to ca. 10 mL. The solid that precipitated was collected by filtration, washed with diethyl ether (4 mL) and dried in vacuo. Yield: 5.20 g (90%); m.p. 187 °C. $C_{35}H_{32}N_4O_4S_2$ (636): calcd. C 66.0, H 5.1, N 8.8, S 10.1; found C 66.1, H 5.1, N 8.7, S 10.2. IR (KBr): $\tilde{\nu} = 1628, 1605$ [s, ν(C=N)], 1339 [s, ν(C−N)], 1285, 1165 [s, ν($SO_2$)] $cm^{-1}$. FAB-MS: *m/z* = 637.3 [$H_3L^+$]. $^1$H NMR (500 MHz, [$D_6$]DMSO): $\delta = 2.09$ (s, 3 H, 10′-H), 2.22 (s, 3 H, 10-H), 5.09 (s, 2 H, 11-H), 6.95−7.0 (m, 4 $H_{arom.}$), 7.10−7.13 (m, 4 $H_{arom.}$), 7.38−7.53 (m, 9 $H_{arom.}$), 7.67 (d, 2 H, 8-H), 7.76 (d, 1 H, 4-H), 8.65 (s, 1 H, 3′-H), 8.88 (s, 1 H, 3-H), 12.82 (s, 1 H, NH), 12.94 (s, 1 H, NH) ppm.

**Synthesis of the Complexes:** All the complexes were obtained by an electrochemical procedure. The cell can be summarised as: Pt(−)|$H_2$ABATs + MeCN|M(+), where M stands for the metal. The synthesis can be typified by the preparation of Cu(ABATs). A suspension of the ligand (0.2 g, 0.32 mmol) in acetonitrile (80 mL), containing tetramethylammonium perchlorate (10 mg), was electrolysed with a current of 10 mA for 3.4 h. Concentration of the resultant solution to a third of its initial volume yielded a yellow-brown solid that was washed with diethyl ether and dried under vacuum. Recrystallisation of the bulk sample by diffusion of diethyl ether into an acetonitrile solution, produced dark-green crystals of [Cu(ABATs)]·0.5$H_2O$ (**4**).

***CAUTION:*** Perchlorate salts are potentially explosive and should therefore be handled with the appropriate care.

The synthetic procedure is the same for all the metals except for manganese and iron. These two compounds were prepared in a closed cell under an argon atmosphere. Prismatic crystals of [Mn(ABATs)]·0.75$H_2O$ (**1**, orange brown), [Fe(ABATs)]·0.75$H_2O$ (**2**, brown), [Ni(ABATs)]·0.75$H_2O$ (**3**, brown), [Cu(ABATs)]·0.5$H_2O$ (**4**, dark green) and [Zn(ABATs)]·0.75$H_2O$ (**5**, yellow) were obtained by slow evaporation of a saturated acetonitrile solution in air. No crystals suitable for X-ray studies could be obtained for [Co(ABATs)] or [Cd(ABATs)].

**[Mn(ABATs)]:** Dark red solid. Yield 0.17 g (78%). $C_{35}H_{30}MnN_4O_4S_2$ (688.9): calcd. C 60.9, H 4.3, N 8.1, S 9.3; found C 60.9, H 4.4, N 8.2, S 9.3. IR (KBr): $\tilde{\nu} = 1632, 1605$ [s, ν(C=N)], 1281 [s, ν(C−N)], 1250, 1127 [s, ν($SO_2$)] $cm^{-1}$. FAB-MS: *m/z* = 690.2 [MnL]$^+$. μ (280 K) = 5.6 BM.

**[Fe(ABATs)]:** Red solid. Yield 0.15 g (70%). $C_{35}H_{30}FeN_4O_4S_2$ (689.5): calcd. C 60.9, H 4.3, N 8.1, S 9.3; found C 60.8, H 4.5, N 8.1, S 9.2. IR (KBr): $\tilde{\nu} = 1636, 1606$ [s, ν(C=N)], 1290 [s, ν(C−N)], 1255, 1136 [s, ν($SO_2$)] $cm^{-1}$. FAB-MS: *m/z* = 691.1 [FeL]$^+$. μ (280 K) = 5.0 BM.

**[Co(ABATs)]:** Dark red solid. Yield 0.17 g (81%). $C_{35}H_{30}CoN_4O_4S_2$ (692.9): calcd. C 60.6, H 4.3, N 8.1, S 9.2; found C 60.7, H 4.4, N 8.0, S 9.2. IR (KBr): $\tilde{\nu} = 1632, 1605$ [s, ν(C=N)], 1285 [s, ν(C−N)], 1258, 1134 [s, ν($SO_2$)], $cm^{-1}$. FAB-MS: *m/z* = 694.1 [CoL]$^+$. μ (280 K) = 4.3 BM.

**[Ni(ABATs)]:** Dark green solid. Yield 0.15 g (72%). $C_{35}H_{30}N_4NiO_4S_2$ (692.7): calcd. C 60.6, H 4.3, N 8.1, S 9.2; found C 60.6, H 4.4, N 8.2, S 9.0. IR (KBr): $\tilde{\nu} = 1640, 1605$ [s, ν(C=N)], 1285 [s, ν(C−N)], 1254, 1138 [s, ν($SO_2$)] $cm^{-1}$. FAB-MS: *m/z* = 693.1 [NiL]$^+$. μ (280 K) = 2.7 BM.

**[Cu(ABATs)]:** Dark green solid. Yield 0.15 g (69%). $C_{35}H_{30}CuN_4O_4S_2$ (697.5): calcd. C 60.2, H 4.3, N 8.0, S 9.2; found C 60.1, H 4.3, N 8.0, S 9.0. IR (KBr): $\tilde{\nu} = 1636, 1605$ [s, ν(C=N)], 1285 [s, ν(C−N)], 1258, 1138 [s, ν(SO$_2$)], cm$^{-1}$. FAB-MS: $m/z$ = 698.2 [CuL]$^+$. μ (280 K) = 2.1 BM.

**[Zn(ABATs)]:** Yellow solid. Yield 0.17 g (80%). $C_{35}H_{30}N_4O_4S_2Zn$ (699.4): calcd. C 60.0, H 4.3, N 8.0, S 9.1; found C 60.1, H 4.3, N 8.1, S 9.2. IR (KBr): $\tilde{\nu}$ = 1643, 1615 [s, ν(C=N)], 1296 [s, ν(C−N)], 1261, 1138 [s, ν(SO$_2$)], cm$^{-1}$. FAB-MS: $m/z$ = 699.1 [ZnL]$^+$. $^1$H NMR (500 MHz, [D$_6$]DMSO): δ = 2.22 (s, 3 H, 10′-H), 2.35 (s, 3 H, 10-H), 4.72 (d, 1 H, 11-H), 5.44 (d, 1 H, 11-H), 6.95−7.03 (m, 3 H, 2 × 9′-H + 6′-H), 7.26−7.38 (m, 7 H, 2 × 9-H + 7-H + 7′-H + 6-H + 5-H + 4′-H + 2′-H), 7.44−7.73 (m, 6 H, 2 × 8′-H + 7-H + 2-H + 1-H + 1′-H), 7.81(d, 1 H, 4-H), 7.90 (d, 2 H, 8-H), 8.75 (s, 1 H, 3′-H), 8.92 (s, 1 H, 3-H) ppm.

**[Cd(ABATs)]:** Pale yellow solid. Yield 0.19 g (83%). $C_{35}H_{30}CdN_4O_4S_2$ (746.4): calcd. C 56.2, H 4.0, N 7.5, S 8.6; found C 56.2, H 3.9, N 7.5, S 8.7. IR (KBr): $\tilde{\nu}$ = 1636, 1613 [s, ν(C=N)], 1289 [s, ν(C=N)], 1258, 1127 [s, ν(SO$_2$)] cm$^{-1}$. FAB-MS: $m/z$ = 749.1 [CdL]$^+$. $^1$H NMR (500 MHz, [D$_6$]DMSO): δ = 2.26 (s, 3 H, 10′-H), 2.28 (s, 3 H, 10-H), 4.97 (br., 2 H, 2 × 11-H), 6.75 (t, 1 H, 5′-H), 6.97 (t, 1 H, 5-H), 7.08−7.16 (m, 6 H, 2 × 9-H + 2 × 9′-H + 6′-H + 7′-H), 7.25 (t, 1 H, 6-H), 7.33−7.36 (m, 2 H, 4′-H + 2′-H), 7.41−7.50 (m, 4 H, 7-H + 2-H + 1-H + 1′H), 7.67 (d, 1 H, 4-H), 7.74 (d, 2 H, 8′H), 7.82 (d, 2 H, 8-H), 8.68 (s, 1 H, 3′-H), 8.70 (s, 1 H, 3-H) ppm.

**Crystallographic Measurements:** Crystals of **1** to **5** suitable for X-ray diffraction studies were obtained as described previously. Data were collected on a Siemens SMART CCD diffractometer for **1**, **2**, **4** and **5** and on a Siemens P4 diffractometer for **3**, with graphite monochromatised Mo-$K_\alpha$ radiation (λ = 0.71073 Å), at room temperature. The structures were solved by direct methods and refined by full-matrix, least-squares based on $F^2$ with the SHELX-97 program package.[32] Absorption corrections were carried out semiempirically from equivalents by use of the Sadabs program.[33] All non-hydrogen atoms were refined anisotropically, except for some of those corresponding to solvated water molecules (**2−4**), which are disordered over two different positions (0.5 and 0.25 occupancies sites) for **1−3** and **5**. Hydrogens bonded to carbon atoms were included in the model at geometrically calculated positions and refined with a riding model. Only some H atoms corresponding to solvated water molecules could be located, fixed and given isotropic displacement parameters of 0.1 Å$^2$.

CCDC-190797−190801 (**1−5**, respectively) contain the supplementary crystallographic data for this paper. These data can be obtained free of charge at www.ccdc.cam.ac.uk/conts/retrieving.html [or from the Cambridge Crystallographic Data Centre, 12, Union Road, Cambridge CB2 1EZ, UK; Fax: (internat.) +44-1223/336-033; E-mail: deposit@ccdc.cam.ac.uk].

---

[1] *Transition Metals in Supramolecular Chemistry* (Eds.: L. Fabrizzi and A. Poggi), Kluwer Academic, Dordecht, **1994**.

[2] J. M. Lehn, *Supramolecular Chemistry-Concepts and Perspectives*, VCH, Weinheim, **1995**.

[3] [3a] E. C. Constable, in *Comprehensive Supramolecular Chemistry, Vol. 9* (Eds.: J. P. Sauvage, M. W. Hosseini), Pergamon, Oxford, **1996**, 213−252. [3b]E. C. Constable, C. E. Housecroft, M. Neuburger, D. Phillips, P. R. Raithby, E. Schofield, E. Sparr, D. A. Tocher, M. Zehnder, Y. Zimmermann, *J. Chem. Soc., Dalton Trans.* **2000**, 2219−2228.

[4] C. Piguet, G. Bernarddinelli, G. Hopfgartner, *Chem. Rev.* **1997**, *97*, 2005−2062.

[5] Y. Zhang, A. Thompson, S. J. Rettig, D. Dolphin, *J. Am. Chem. Soc.* **1998**, *120*, 13537−13538.

[6] [6a] P. N. W. Baxter, J. M. Lehn, K. Rissanen, *Chem. Commun.* **1997**, 1323−1324. [6b] K. M. Gardinier, R. G. Khoury, J. M. Lehn, *Chem. Eur. J.* **2000**, *6*, 4124−4131.

[7] [7a] J. S. Fleming, K. L. V. Mann, S. M. Couchman, J. C. Jeffery, J. A. McCleverty, M. D. Ward, *J. Chem. Soc., Dalton Trans.* **1998**, 2047−2052. [7b] C. R. Rice, S. Wörl, J. C. Jeffery, R. L. Paul, M. D. Ward, *J. Chem. Soc., Dalton Trans.* **2001**, 550−559.

[8] G. Baum, E. C. Constable, D. Fenske, C. E. Housecroft, T. Kulke, M. Neuburger, M. Zehnder, *Chem. Eur. J.* **2000**, *6*, 4510−4517.

[9] [9a] C. Piguet, *J. Incl. Phenom. Macrocycl. Chem.* **1999**, *34*, 361−391. [9b] G. Muller, J. C. G Bunzli, K. J. Schenk, C. Piguet, G. Hopfgartner, *Inorg. Chem.* **2001**, *40*, 2642−2651.

[10] [10a] M. Albrecht, *Chem. Soc. Rev.* **1998**, *27*, 281−288. [10b] M. Albrecht, O. Blau, H. Röttele, *New J. Chem.* **2000**, *24*, 619−622.

[11] O. Mamula, A. von Zelewsky, T. Bark, G. Bernardinelli, *Angew. Chem. Int. Ed. Eng.* **1999**, *38*, 2945−2948.

[12] [12a] L. Zhu, Y-X. Tong, X-M. Cheng, *J. Chem. Soc., Dalton Trans.* **2000**, 4182−4186. [12b] G. Yang, S. L. Zheng, X-M. Chen, H. K. Lee, Z-Y. Zhou, T. C. W. Mak, *Inorg. Chim. Acta* **2000**, *303*, 86−93.

[13] G. C. van Stein, G. van Koten, K. Vrieze, C. Brevard, A. L. Spek, *J. Am. Chem. Soc.* **1984**, *106*, 4486−4492.

[14] P. K. Boyer, K. A. Porter, A. D. Rae, A. C. Willis, B. Wild, *Chem. Commun.* **1998**, 1153−1154.

[15] [15a] M. J. Hannon, C. L. Painting, A. Jackson, J. Hamblin, W. Errington, *Chem. Commun.* **1997**, 1807−1808. [15b] M. J. Hannon, S. Bunce, A. J. Clarke, N. W. Alcock, *Angew. Chem. Int. Ed.* **1999**, *38*, 1277−1278. [15c] L. J. Chields, N. W. Alcock, M. J. Hannon, *Angew. Chem. Int. Ed.* **2001**, *40*, 1079−1081.

[16] V. Amendola, L. Fabbrizzi, L. Linati, C. Mangano, P. Pallavicini, V. Pedrazzini, M. Zema, *Chem. Eur. J.* **1999**, *5*, 3679−3688.

[17] H. Cheng, D. Chun-Ying, F. Chen-Jie, M. Qing-Jin, *J. Chem. Soc., Dalton Trans.* **2000**, 2419−2424.

[18] [18a] N. Yoshida, K. Ichikawa, *Chem. Commun.* **1997**, 1091−1092. [18b] N. Yoshida, H. Oshio, T. Ito, *Chem. Commun.* **1998**, 63−64. [18c] N. Yoshida, K. Ichikawa, M. Shiro, *J. Chem. Soc., Perkin Trans.* **2000**, 17−26.

[19] L. Carbonaro, M. Isola, V. Liuzzo, F. Marchetti, F. Balzano, C. S. Pomelli, A. Raffaelli, *Eur. J. Inorg. Chem.* **2001**, 353−357.

[20] [20a] J. Sanmartín, M. R. Bermejo, A. M. García-Deibe, O. Piro, E. E. Castellano, *Chem. Commun.* **1999**, 1953−1954. [20b] J. Sanmartín, M. R. Bermejo, A. M. García-Deibe, A. L. Llamas-Saiz, *Chem. Commun.* **2000**, 795−796.

[21] [21a] M. Vázquez, M. R. Bermejo, M. Fondo, A. M. González, J. Mahía, L. Sorace, D. Gatteschi, *Eur. J. Inorg. Chem.* **2001**, 1863−1868. [21b] M. Vázquez, M. R. Bermejo, M. Fondo, A. García- Deibe, A. M. González, R. Pedrido, *Eur. J. Inorg. Chem.* **2002**, 465−472.

[22] [22a] M. Vázquez, M. R. Bermejo, M. Fondo, A. M. García-Deibe, A. M. González, R. Pedrido, J. Sanmartín, *Z. Anorg. Allg. Chem.* **2002**, *628*, 1068−1074. [22b] M. Vázquez, M. R. Bermejo, J. Sanmartin, A. M. Garcia-Deibe, C. Lodeiro, J. Mahia, *J. Chem. Soc., Dalton Trans.* **2002**, 870−877.

[23] M. A. Torzilli, S. Colquhoun, J. Kim, R. H. Beer, *Polyhedron* **2002**, *21*, 705−713.

[24] [24a] M. R. Bermejo, A. Sousa, M. Fondo, M. Helliwell, *New. J. Chem.* **2000**, *24*, 33−41. [24b] A. Sousa, M. R. Bermejo, M. Fondo, A. García-Deibe, A. Sousa-Pedrares, O. Piro, *New J. Chem.* **2001**, *25*, 647−654.

[25] M. Morioka, M. Kato, H. Yoshida, T. Ogata, *Heterocycles* **1997**, *45*, 1173−1181.

[26] K. Nakamoto, in *Infrared and Raman Spectra of Inorganic and Coordination Compounds*, John Wiley & Sons, New York, **1997**.

[27] J. S. Griffith, "*The Theory of Transition Metal Ions*", Cambridge University Press, Cambridge, **1961**.

[28] M. J. Knapp, J. Krzystek, L. C. Brunel, D. N Hendrickson, *Inorg. Chem.* **2000**, *39*, 281−288.

[29] A. Bencini, D. Gatteschi, in *Transition Metal Chemistry* (Eds.:

B. N. Figgis, G. Melson) vol. 8, p. 1, Marcel Dekker, New York, **1982**.

[30] N. I. Chernova, Y. S. Ryabokobylky, V. G. Brudz, B. M. Bolotin, *Zh. Neorg. Khim.* **1971**, 1680−1684.

[31] J. Mahia, M. Maestro, M. Vázquez, M. R. Bermejo, A. M. Gonzalez, M. Maneiro, *Acta Crystallogr., Sect. C* **1999**, *C55*, 2158−2160.

[32] G. M. Sheldrick, SHELX-97 (SHELXS 97 and SHELXL 97), Programs for Crystal Structure Analyses, University of Göttingen, Germany, **1998**.

[33] SADABS, Area-Detector Absorption Correction. Siemens Industrial Automation Inc., Madison, WI, **1996**.

Received October 8, 2002
[I02557]